Lung Cancer 184 (2023) 107345

Contents lists available at ScienceDirect

Lung Cancer

journal homepage: www.elsevier.com/locate/lungcan

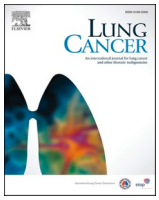

Clinical implication of the 2020 International Association for the Study of Lung Cancer histologic grading in surgically resected pathologic stage 1 lung adenocarcinomas: Prognostic value and association with computed tomography characteristics

In Sung Cho [a], Hyo Sup Shim [b], Hye-Jeong Lee [a], Young Joo Suh [a,*]

[a] Department of Radiology, Research Institute of Radiological Science, Center for Clinical Imaging Data Science, Severance Hospital, Yonsei University College of Medicine, Seoul, Republic of Korea
[b] Department of Pathology, Yonsei University College of Medicine, Seoul, Republic of Korea

ARTICLE INFO

Keywords:
Lung adenocarcinoma
Prognosis
CT characteristics
Histologic subtype

ABSTRACT

Objectives: To investigate the incremental prognostic value of the 2020 International Association for the Study of Lung Cancer (IASLC) histologic grading system over traditional prognosticators in surgically resected pathologic stage 1 lung adenocarcinomas and to identify the clinical and radiologic characteristics of lung adenocarcinomas reclassified by the 2020 histologic grading system.
Materials and methods: We retrospectively enrolled 356 patients who underwent surgery for pathologic stage 1 adenocarcinoma between January 2016 and December 2017. The histologic grading was classified according to the predominant histologic subtype (conventional system) and the updated 2020 IASLC grading system. The clinical and computed tomography (CT) characteristics were compared according to the reclassification of the updated system. The performance of prognostic models for recurrence-free survival based on the combination of pathologic tumor size, histologic grade, and CT-based information was compared using the c-index.
Results: Postoperative recurrence occurred in 6.7% of patients during the follow-up period (mean, 1589.2 ± 406.7 days). Fifty-nine of 244 (24.2%) tumors with intermediate grades in the conventional system were reclassified as grade 3 with the updated grading system. They showed significantly larger solid proportions and higher percentages of pure solid nodules on CT compared to tumors without reclassification ($n = 185$) ($P < 0.05$). Prognostic prediction models based on pathology tumor size and histologic grades had significantly higher c-indices (0.754–0.803) compared to the model based on pathologic tumor size only (c-index:0.723, $P < 0.05$).
Conclusion: The 2020 IASLC histologic grading system has significant incremental prognostic value over the pathologic stage in surgically resected pathologic stage 1 lung adenocarcinoma. Reclassified lung adenocarcinomas using the updated grading system have a larger solid proportion and a higher percentage of pure solid nodules on CT.

1. Introduction

Lung cancer is the main cause of cancer-related mortality worldwide, and the incidence of adenocarcinoma continues to increase [1–3]. The clinical or pathological tumor stage is a traditional and well-established prognostic marker for overall survival or recurrence-free survival (RFS) [4]. In addition to the tumor stage, the histologic subtype of lung adenocarcinoma is an independent prognostic indicator, including the early stage of tumors [5,6].

Lung adenocarcinomas have heterogeneity in their histologic background and show multiple combinations of histologic patterns and proportions. The classification of the histologic subtype of lung adenocarcinoma has been proposed by the International Association for the Study of Lung Cancer (IASLC)/the American Thoracic Society (ATS)/the European Respiratory Society (ERS) in 2011 [7]. Several studies have suggested that a histologic grading system that classifies tumors into

* Corresponding author at: Department of Radiology, Severance Hospital, Research Institute of Radiological Science, Center for Clinical Imaging Data Science, Yonsei University College of Medicine, 50-1 Yonsei-ro, Seodaemun-gu, Seoul 03722, Republic of Korea.
E-mail address: rongzusuh@gmail.com (Y.J. Suh).

https://doi.org/10.1016/j.lungcan.2023.107345
Received 13 March 2023; Received in revised form 21 June 2023; Accepted 10 August 2023
Available online 12 August 2023

three histologic grades based on the most predominant histologic subtype has provided prognostic stratification in lung adenocarcinomas [5,8,9]. Nevertheless, there is a growing need for a better grading scheme for the prognostication of lung adenocarcinomas. Recently, a new grading system for non-mucinous, invasive adenocarcinoma was proposed by the IASLC in 2020 and included a combination of predominant histologic subtypes with a percentage of high-grade (solid, micropapillary, or complex glandular) patterns [10].

The utility of computed tomography (CT) parameters (e.g., lesion type or ground-glass opacity [GGO] ratio) has been investigated for their prognostic value in lung adenocarcinoma or association with histologic grades classified by predominant histologic patterns [11–16]. Because the new grading system has been proposed to improve prognostication using histologic subtype information, some adenocarcinomas with high-grade patterns are expected to be reclassified when assessed using the updated grading system. Although previous studies have validated the prognostic value of the new histologic grading system [17,18], its incremental prognostic value compared to the conventional histologic grade has not been widely investigated in various populations. In addition, the clinical and radiologic characteristics of tumors that are reclassified as having different categories in the updated system have not been investigated.

The purposes of our study were to investigate the incremental prognostic value of the updated histologic subtype classification over traditional prognosticators in surgically resected pathologic stage 1 lung adenocarcinoma and to identify the clinical and radiologic characteristics of lung adenocarcinomas that were reclassified using the updated histologic grading system.

2. Materials and methods

2.1. Patients

This study was approved by the Institutional Review Board of our institution, and the requirement for informed consent was waived because of the retrospective nature of the study. From our surgical database, 587 patients who underwent surgical resection for lung adenocarcinoma between January 2016 and December 2017 were retrospectively enrolled (Fig. 1). Among those patients, some were excluded for the following reasons: 1) preoperative clinical stage was more advanced than stage 1 (n = 132); 2) pathologic stage was more advanced than stage 1 (n = 34); 3) patients with adenocarcinoma in situ or minimally invasive adenocarcinoma (n = 17), invasive mucinous adenocarcinoma (n = 33), unavailable histologic subtype classification (n = 4), or recurrent or metastatic lesions from previous malignancy (n = 3) on surgical pathology; 4) patients with suboptimal CT image quality or undefinable margin of CT lesions (n = 6) or without available preoperative CT examination (n = 1); and 5) patients who received preoperative chemoradiotherapy (n = 1). Finally, 356 patients were included in the study.

2.2. Clinical data collection

Data on clinical characteristics, including sex, age, and smoking history, were collected from preoperative clinical records. Smoking history was classified into three groups: never, former, and current smokers. The occurrence and date of postoperative recurrence were investigated until the clinical follow-up end date of February 21, 2022 (mean postoperative follow-up period, 1589.2 ± 406.7 days). Recurrence was defined as disease appearance at either intrapulmonary or extrapulmonary distant sites after at least 3 months of the disease-free interval between lung cancer surgery and recurrence. The date of recurrence was defined as the date of the first examination on which recurrence was suspected.

2.3. CT examinations

For all patients, preoperative chest CT scans were performed using one of the following multi-detector row scanners: Somatom Sensation 16, Somatom Sensation 64, Definition Flash (Siemens Medical Solutions, Forchheim, Germany), Discovery CT 750 HD, Revolution (GE Medical Systems, Milwaukee, Wisconsin, USA), or iCT (Philips Medical Systems, the Netherlands). Details of the scanning parameters were the same as those described previously [19]. Axial, coronal, and sagittal images were reconstructed with soft tissue kernel and a slice thickness of 1–1.25 mm for the axial plane and 3 mm for the coronal and sagittal planes. All the CT datasets were transferred to a picture archiving and communication system.

2.4. CT image analysis

Preoperative chest CT images were reviewed by a thoracic radiologist (with 13 years of experience in chest CT examination), who was blinded to the clinical and pathological information. CT image analysis included an assessment of the CT lesion type and measurement of the lesion size. The largest longitudinal diameters of the entire tumor and the inner solid portion were measured on cross-sections (axial, coronal, or sagittal planes) in the lung window setting. We defined the solid component as an increased opacity that obscured adjacent vascular structures. CT lesion type was classified into four categories according to the proportion of intralesional solid components: pure ground-glass nodule (GGN) (solid component, 0%), GGO-dominant part-solid nodule (PSN) (0 < solid component < 50%), solid-dominant PSN (50 ≤ solid component < 100%), and pure solid nodule (solid component, 100%) [20]. The proportion of solid components was calculated as the ratio of the maximal solid diameter to that of the total tumor.

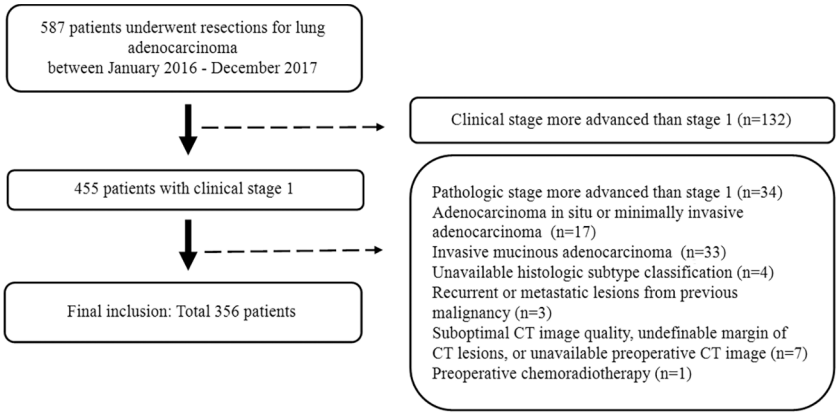

Fig. 1. Flow chart of the study population.

2.5. Histologic evaluation

Pathological information was collected from the surgical pathological reports. One board-certified thoracic pathologist evaluated the histologic subtypes with a semiquantitative estimation of all patterns in 5% increments, as suggested by the 2015 WHO classification of lung tumors [21]. According to the information about the histologic subtype of the tumor in the pathologic report, histologic grades were classified in two ways: according to the predominant histologic subtype (the conventional grading system) [21] and the updated IASLC grading system [10]. In the conventional grading system, tumors were classified into one of three categories: low-grade (lepidic predominant), intermediate-grade (acinar or papillary predominant), or high-grade (solid or micropapillary predominant). For the updated grading system, tumors were classified into one of three categories: grade 1 (lepidic predominant with no or<20% of high-grade patterns); grade 2 (acinar or papillary predominant tumor, both with no or<20% of high-grade patterns [solid, micropapillary, or complex glandular]); and grade 3 (any tumor with 20% or more of high-grade patterns). The tumor stage was assessed according to the 8th edition of the TNM classification for lung cancer [22]. The presence of lymphovascular invasion and spread through air spaces were also assessed. Further, the mutation status of epidermal growth factor receptor mutations in the tumors was examined.

2.6. Outcomes

The primary outcome of this study was the postoperative recurrence. Recurrence after surgery was assessed based on follow-up medical records and imaging study results. The secondary outcome was the reclassification of histologic grading on the updated histologic grading system and the characteristics of tumors with reclassification. Reclassification was defined as the classification of the tumor as higher or lower than the conventional grading system (e.g., intermediate grade on the conventional system and grade 3 on the updated system).

2.7. Statistical analysis

All statistical analyses were performed using SPSS software, version 25 (SPSS, Chicago, IL, USA); MedCalc for Windows, version 20.115 (MedCalc Software, Mariakerke, Belgium); and R package, version 4.1.2 (R Foundation for Statistical Computing, Vienna, Austria). Normally distributed data were identified using the Shapiro–Wilk test. Continuous variables were presented as mean ± standard deviation and were compared using the independent *t*-test for normally distributed data or the Mann–Whitney *U* test for non-normally distributed data. The relationship between CT lesion type and histologic grading system was analyzed using the chi-squared test. Clinical and CT characteristics according to tumor recurrence and reclassification of the updated system were compared using the chi-squared or Fischer's exact test for categorical variables and independent *t*-test or the Mann–Whitney *U* test for continuous variables. RFS was presented using Kaplan–Meier curves, and the differences between groups that were classified by histologic grading were analyzed using the log-rank test. The restricted mean survival time (RMST) was compared between the groups at postoperative time points of 2 and 4 years. Cox proportional hazard analysis was performed to identify significant predictors of RFS. We built four different prognostic prediction models: Model 1, based on the pathologic tumor size; Model 2, based on the conventional grading system combined with the pathologic tumor size; Model 3, updated histologic grading with the pathologic tumor size; and Model 4, based on the solid portion on CT and CT lesion type. For Models 2 and 3, the second category (intermediate grade in the conventional system and grade 2 in the updated system) was set as the reference group because recurrence was not observed in the first category (lowest grade) in both systems. The performance of each model was assessed and compared using Harrell's c-index. To evaluate the discriminatory function of each model, the time-dependent receiver operating characteristic curve method was used, and the integrated area under the curve (iAUC) was calculated to compare the predictive accuracy of the models. The iAUC is a weighted average of the AUC across a follow-up period and a measure of the predictive prognosis of the model during follow-up, with a higher iAUC indicating a better predictive prognosis. Differences in the c-index and iAUC between the models were calculated using a bootstrapping method with a resampling of 1000 times. P-values<0.05 were considered statistically significant.

3. Results

3.1. Patients and tumor lesion characteristics

The study population consisted of 356 patients (150 men, mean age 70.1 ± 9.5 years), and their clinical characteristics are shown in Table 1. Most (66.9%) of the included patients had never smoked. The size of the entire lesion and solid portion on CT averaged 20.8 ± 7.3 mm and 13.5 ± 7.3 mm, respectively. In terms of CT lesion type, there were five pure GGNs (1.4%), 110 GGO-dominant PSNs (30.9%), 150 solid-dominant PSNs (42.1%), and 91 pure solid nodules (25.6%). The predominant histologic subtypes were lepidic in 93 patients (26.1%), acinar in 206 (57.9%), papillary in 38 (10.7%), solid in 15 (4.2%), and micropapillary in four (1.1%). During the follow-up period (mean 1589.2 ± 406.7 days), tumor recurrence occurred in 6.7% (24 of 356) of the patients.

3.2. Histologic grades assessed by the conventional and updated histologic grading systems

When applying the conventional grading system, tumors were classified as low, intermediate, and high grades in 93 (26.1%), 244 (68.5%), and 19 (5.3%) patients, respectively (Table 1). When applying the updated grading system, tumors were classified as grade 1, 2, and 3 in 93 (26.1%), 185 (52.0%), and 78 (21.9%) patients, respectively. Fifty-nine of 244 (24.2%) tumors with intermediate grades in the conventional system were reclassified as grade 3 using the updated grading system (Supplementary Table 1). None of the tumors with low or high histologic grades were reclassified.

CT lesion type and histologic grade showed significant associations in both systems ($P < 0.001$, Supplementary Table 2). In both grading systems, tumors in the higher category tended to have a significantly larger solid portion on CT ($P < 0.001$). Among the 59 tumors showing reclassification, 32 (54.2%) had a CT lesion type of pure solid nodule, 22 (37.3%) had solid-dominant PSNs, and 5 (8.5%) had GGO-dominant PSNs (Table 2). Among tumors with the intermediate grade on the conventional system, tumors that were reclassified on the updated system ($n = 59$) showed a significantly larger solid proportion and a higher percentage of pure solid nodules on CT, higher rate of presence of lymphovascular invasion or spread through air spaces, and wild-type epidermal growth factor receptor mutation, compared to tumors without reclassification ($n = 185$) ($P < 0.05$, Figs. 2 and 3). The tumor recurrence rate was higher in reclassified tumors (16.9% vs. 5.9%, $P = 0.009$).

3.3. Comparison of tumor characteristics according to the postoperative recurrence

The size of the total lesion and solid portion on CT was significantly larger in the recurrence group than in the non-recurrence group ($P < 0.001$ for both; Table 1). Tumors in the recurrence group had the most frequent CT lesion type as a pure solid nodule (66.7%), whereas solid-dominant PSN was the most common CT lesion type in the non-recurrence group ($P < 0.001$). The distribution of the predominant histologic subtype was different between the recurrence and non-recurrence groups. The acinar type was the most common

Table 1
Clinical characteristics of the study population.

	Entire study population (n = 356)	No recurrence (n = 332)	Recurrence (n = 24)	P value
Age	70.1 ± 9.5	70.0 ± 9.5	72.4 ± 9.4	0.237
Male sex	150 (42.1)	142 (42.8)	8 (33.3)	0.367
Smoking history				0.488
Never smoker	238 (66.9)	220 (66.3)	18 (75)	
Former smoker	102 (28.7)	98 (29.5)	4 (16.7)	
Current smoker	16 (4.5)	14 (4.2_	2 (8.3)	
CT total size (mm)	20.8 ± 7.3	20.6 ± 7.3	23.9 ± 6.3	0.03
CT solid size (mm)	13.5 ± 7.3	12.9 ± 7.2	20.8 ± 4.9	<0.001
CT solid proportion (%)	65.2 ± 28.4	63.5 ± 28.2	89.7 ± 17.7	<0.001
CT lesion type				<0.001
Pure GGN	5 (1.4)	5 (1.5)	0 (0)	
GGO-dominant PSN	110 (30.9)	109 (32.8)	1 (4.2)	
Solid-dominant PSN	150 (42.1)	143 (43.1)	7 (29.2)	
Pure solid	91 (25.6)	75 (22.6)	16 (66.7)	
Pathologic tumor size (cm)	1.6 ± 0.9	1.6 ± 0.9	2.4 ± 0.6	<0.001
Pathologic tumor size				<0.001
Size ≤ 1 cm	96 (27.0)	96 (28.9)	0 (0)	
1 cm < size ≤ 2 cm	138 (38.8)	1131 (39.5)	7 (29.2)	
2 cm < size	122 (34.3)	105 (31.6)	17 (70.8)	
Predominant histologic subtype				0.001
Lepidic	93 (26.1)	93 (28)	0 (0)	
Acinar	206 (57.9)	189 (56.9)	17 (70.8)	
Papillary	38 (10.7)	34 (10.2)	4 (16.7)	
Solid	15 (4.2)	13 (3.9)	2 (8.3)	
Micropapillary	4 (1.1)	3 (0.9)	1 (4.2)	
Conventional histologic grade				0.001
Low grade	93 (26.1)	93 (28)	0 (0)	
Intermediate grade	244 (68.5)	223 (67.2)	21 (87.5)	
High grade	19 (5.3)	16 (4.8)	3 (21.5)	
Updated histologic grade				<0.001
Grade 1	93 (26.1)	93 (28)	0 (0)	
Grade 2	185 (52.0)	174 (52.4)	11 (45.8)	
Grade 3	78 (21.9)	65 (19.6)	13 (54.2)	
Lymphovascular invasion				<0.001
Absent	333 (93.5)	317 (95.5)	16 (66.7)	
Present	23 (6.5)	15 (4.5)	8 (33.3)	
Spread through air spaces				<0.001
Absent	248 (69.7)	241 (72.6)	7 (29.2)	
Present	108 (30.3)	91 (27.4)	17 (70.8)	
EGFR mutation				0.646
Wild type	120 (33.7)	111 (33.4)	9 (37.5)	
Mutation	233 (65.4)	218 (65.7)	15 (62.5)	
Not available	3 (0.8)	3 (0.9)	0 (0)	
Type of surgery				0.790
Lobectomy	261 (73.3)	242 (72.9)	19 (79.2)	
Segmentectomy	34 (9.6)	33 (9.9)	1 (4.2)	
Wedge resection	59 (16.6)	55 (16.6)	4 (16.7)	
Pneumonectomy	2 (0.6)	2 (0.6)	0 (0)	

CT: Computed tomography, GGN, ground-glass nodule; GGO: Ground-glass opacity, PSN: Part-solid nodule; EGFR, epidermal growth factor receptor.

predominant histologic type in both the recurrence and non-recurrence groups (70.8% and 56.9%), but the proportion of solid or micropapillary predominant histologic type was significantly higher in the recurrence group (12.5% vs. 4.8%). Further, the pathologic tumor size tended to be significantly larger in the recurrence group than in the non-recurrence group (P < 0.001).

Table 2
Comparison of clinical, radiologic, and pathologic characteristics according to the reclassification of histologic grading among patients with tumors of intermediate grades on the conventional grading system.

	Reclassification (n = 59)	No reclassification (n = 185)	P value
Age	70.5 ± 11.2	69.6 ± 9.5	0.550
CT total size (mm)	20.3 ± 6.3	22.1 ± 7.8	0.108
Solid portion size on CT (mm)	17.2 ± 6.5	15.1 ± 7.0	0.044
Solid portion size on CT			0.153
Size ≤ 1 cm	10 (16.9)	55 (29.7)	
1 cm < size ≤ 2 cm	31 (52.5)	81 (43.8)	
2 cm < size	18 (30.5)	49 (26.5)	
CT solid proportion (%)	85.1 ± 20.4	69.4 ± 25.1	<0.001
CT lesion type			<0.001
Pure GGN	0 (0)	1 (0.5)	
GGO-dominant PSN	5 (8.5)	40 (21.6)	
Solid-dominant PSN	22 (37.3)	101 (54.6)	
Pure solid nodule	32 (54.2)	43 (23.2)	
Pathologic tumor size (cm)	1.9 ± 0.6	2.0 ± 0.7	0.357
Pathologic tumor size			0.617
Size ≤ 1 cm	3 (5.1)	5 (2.7)	
1 cm < size ≤ 2 cm	31 (52.5)	94 (50.8)	
2 cm < size	25 (42.4)	86 (46.5)	
Predominant histologic subtype			0.798
Acinar	49 (83.1)	157 (84.9)	
Papillary	10 (16.9)	28 (15.1)	
Lymphovascular invasion			<0.001
Absent	44 (74.6)	181 (97.8)	
Present	15 (25.4)	4 (2.2)	
Spread through air spaces			<0.001
Absent	16 (27.1)	138 (74.6)	
Present	43 (72.9)	47 (25.4)	
EGFR mutation			0.042
Wild type	27 (45.8)	53 (28.6)	
Mutation	32 (54.2)	130 (70.3)	
Not available	0 (0)	2 (1.1)	
Recurrence	10 (16.9)	11 (5.9)	0.009

CT: computed tomography; EGFR, epidermal growth factor receptor; GGN, ground-glass nodule; GGO: ground-glass opacity; PSN: part-solid nodule.

3.4. Survival analysis for recurrence-free survival

The Kaplan–Meier survival curves demonstrated the RFS of patients with tumors of each histologic grade according to both conventional and updated histologic grading systems (P value for log-rank test < 0.05 for both grading systems; Fig. 4). At the time point of the 4-year follow up, the RMST was not significantly different between the intermediate and high grades in the conventional grading system (difference of survival time: 100.4 days, P = 0.219). However, the RMST at postoperative 4 years was significantly different between grade 2 and 3, on the updated grading system (difference of survival time: 111.4 days, P = 0.004). The RMST of the grade 1 and 2 on the updated grading system and that of the intermediate and high grades in the conventional grading system at the time point of the 2-year follow up were not statistically significant.

3.5. Prognostic model for the prediction of tumor recurrence

In the univariable Cox regression analysis, a larger solid portion on CT, CT lesion type, higher histologic grade on updated systems, and larger pathologic tumor size were associated with tumor recurrence (P < 0.05, Table 3). Age, sex, and histologic grade on conventional system were not significantly associated with the RFS (P > 0.05).

Prognostic prediction models based on the multivariable Cox regression analysis showed that Models 2 and 3, which were based on the pathologic tumor size and histologic grades, had significantly higher c-indices (0.754 [95% CI 0.684–0.82] and 0.803 [95% CI 0.734–0.86]

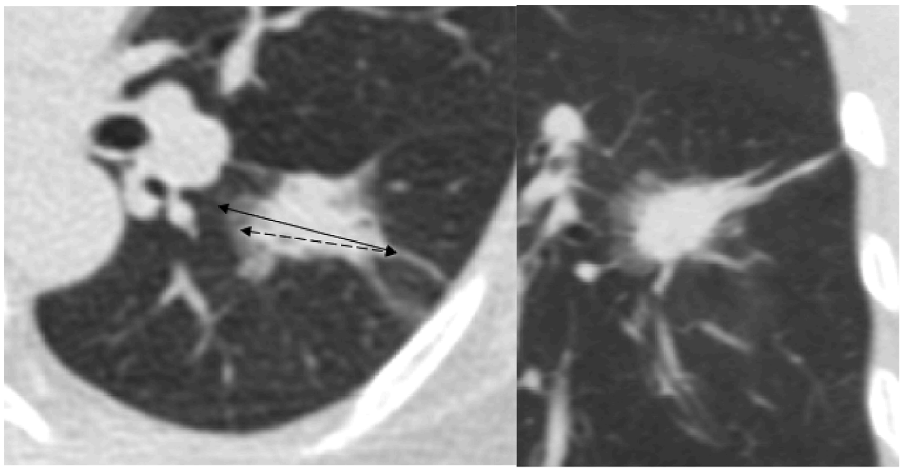

Fig. 2. A representative case of a lung adenocarcinoma that was reclassified on the updated classification. (A, B) The axial and coronal non-contrast chest computed tomography (CT) images of a 63-year-old female patient show a 3.0 cm part-solid mass (solid portion, 2.8 cm) in her left lower lobe with pleural tagging. On surgical pathology, the lesion was confirmed as an invasive adenocarcinoma with histologic subtype components of acinar (70%), micropapillary (20%), and lepidic (10%), indicating intermediate grade on the conventional classification and grade 3 on the updated classification. (C) In the follow-up CT after 4 years, a protruding soft tissue lesion (arrow) was newly observed at the left main bronchus, (D) which was confirmed as a recurred tumor via bronchoscopic biopsy.

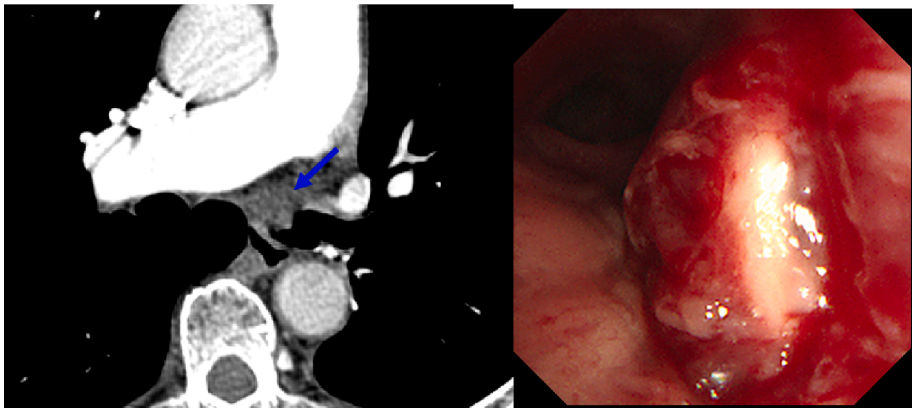

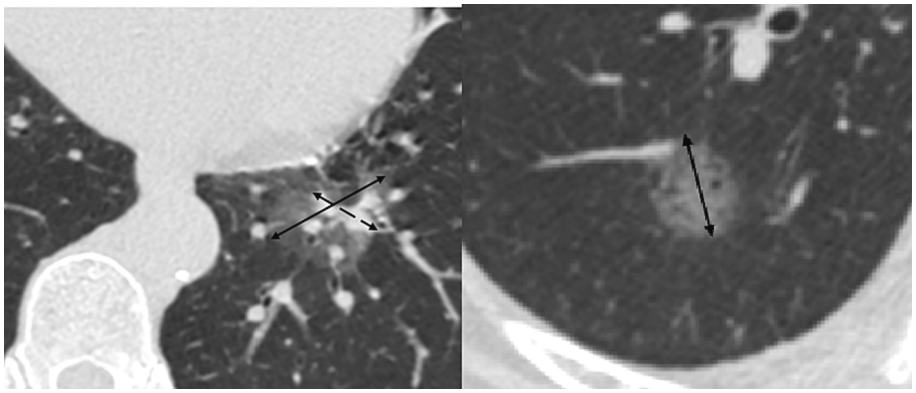

Fig. 3. Cases of lung adenocarcinomas that were not reclassified on the updated classification. (A) The axial non-contrast chest computed tomography (CT) of a 67-year-old female patient shows a 3.6 cm, ground-glass opacity-dominant part-solid mass (solid portion 1.7 cm) in her left lower lobe. On surgical pathology, the lesion was confirmed as an invasive adenocarcinoma with histologic subtype components of acinar (70%) and lepidic (30%), indicating an intermediate grade on the conventional classification and grade 2 on the updated classification. (B) The axial non-contrast chest CT of a 67-year-old female patient shows a 1.7 cm, pure ground-glass nodule in the right lower lobe, which was confirmed as an invasive adenocarcinoma with acinar (60%) and lepidic (40%) subtypes on surgical pathology. At the postoperative follow-ups after 2099 and 2138 days for each, no tumor recurrence occurred in either patient.

respectively) and iAUC (0.751 [95% CI 0.69–0.81] and 0.796[95% CI 0.733–0.857], respectively), compared to Model 1 based on the pathologic tumor size only (c-index: 0.723 [95% CI 0.652–0.792]; iAUC, 0.731 [95% CI 0.663–0.796]) (Tables 4 and 5). This indicated that both conventional and updated histologic grading systems had incremental prognostic value for the tumor size. Models 2 and 3 showed no statistically significant differences in the c-indices and iAUCs. Model 4 based on the solid proportion on CT and CT lesion type, showed a c-index of 0.815 (95% CI 0.739–0.884) and iAUC of 0.81 (0.736–0.879) for prediction of the RFS, and the c-index was significantly higher than that of Model 1 (Tables 4 and 5). Model 4 showed higher c-index than Models 2 and 3; however, the difference was statistically insignificant (Table 5).

4. Discussion

Our study demonstrates that the histologic grades of lung adenocarcinomas on both conventional and updated grading systems have a significant incremental prognostic value on the tumor stage for predicting RFS in patients who undergo surgical resection for pathologic stage 1 lung adenocarcinoma. The c-indices of prognostic models based on the pathologic tumor size and histologic grades assessed by conventional and updated grading systems were 0.754 and 0.803,

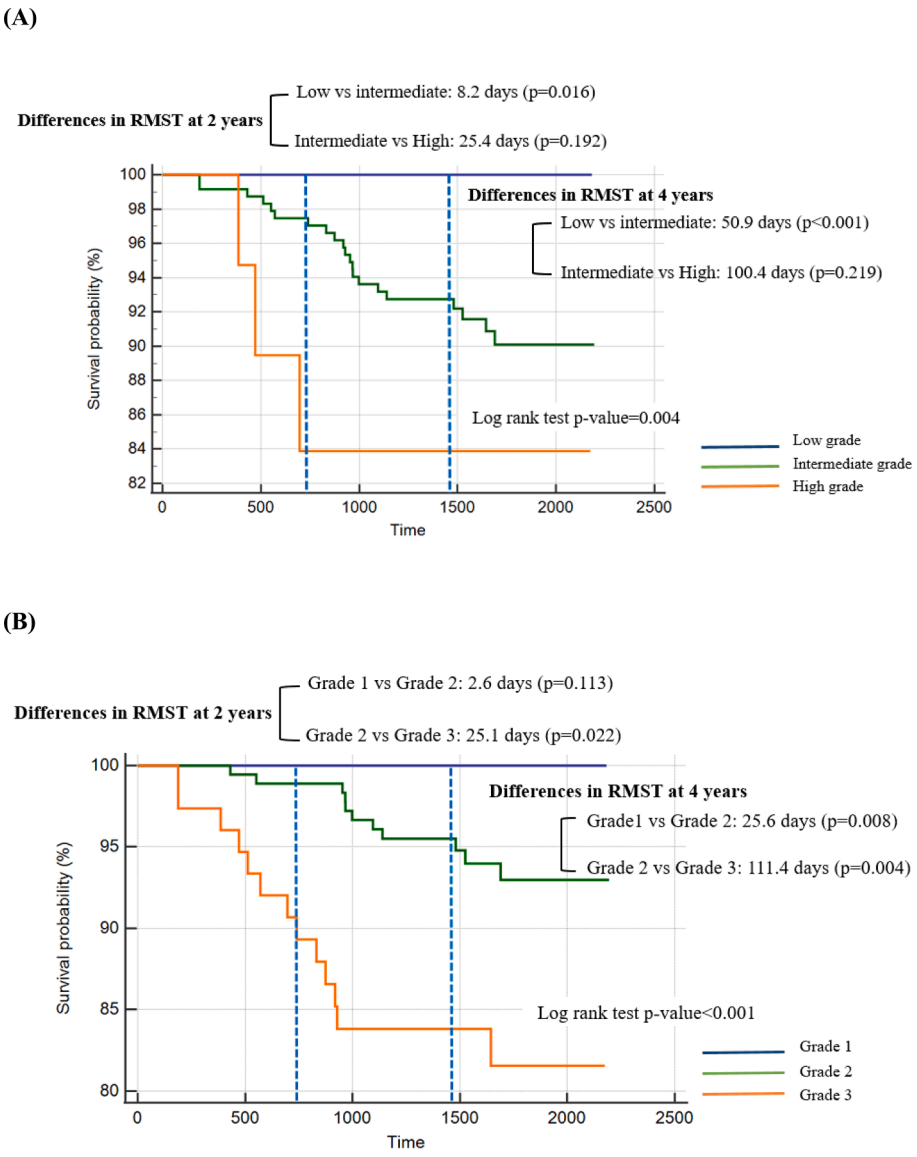

Fig. 4. Kaplan–Meier curves for recurrence-free survival (RFS) with restricted mean survival time (RMST) in (A) the conventional grading system and (B) the updated grading system.

respectively, which were higher than the c-index (0.723) of the model based on the pathologic tumor size alone. Approximately 24% of tumors with the intermediate grade on the conventional grading system are reclassified as grade 3 on the updated grading system, and they had different lesion characteristics, such as a larger solid portion and a higher percentage of pure solid nodules on CT, and higher tumor recurrence rate, compared to tumors without reclassification.

A new histologic grading for non-mucinous, invasive lung adenocarcinoma has been proposed by the IASLC to provide better prognostic stratification, in which the primary changes are the introduction of a complex glandular pattern and the application of a 20% cutoff for high-grade patterns. A few previous studies have validated the updated histologic grading system, mostly in East Asian patients with surgically resected early adenocarcinomas [17,23–25]. The new grading system has been reported to have incremental prognostic value compared with conventional prognosticators, such as tumor stage for the RFS or overall survival. It has also provided a slightly higher performance than the conventional tumor grading system based on the predominant histologic subtype [17,18,23,25]. Our study results are consistent with those of previous studies: 1) the prognostic model based on the tumor stage (size) and updated histologic grading system had added prognostic value to the model based on the tumor stage only; 2) the c-index of the prognostic value of the model was higher than that of the model based on the tumor stage and conventional histologic grading system, even though statistical significance was not reached. In addition, at 4 years postoperatively, grades 2 and 3 in the updated grading system showed significantly different RMSTs, whereas the intermediate grade and high grade in the conventional system did not show a statistical difference. While this difference in RMST could be due to the small number of high-grade tumor and low recurrence rate, the update grading system may provide the better stratification for predicting long-term prognosis after surgery.

The improved prognostic value of the updated grading system may be attributable to better prognostic stratification in patients with tumors showing reclassification. In our study, 24.2% of the tumors with intermediate grade (acinar or papillary predominant tumors) in the conventional grading system had > 20% high-grade patterns as the non-predominant histologic subtype and were reclassified to a higher category (grade 3) on the updated system. These tumors showed a higher recurrence rate (16.9% vs. 5.9%) and a higher proportion of other adverse pathologic prognosticators, such as lymphovascular invasion or spread through air spaces. Notably, none of the tumors with lepidic

Table 3
Univariable Cox-regression analysis for recurrence-free survival.

	HR	95% CI	P value
Age (per 1-year increase)	1.032	0.986–1.080	0.176
Sex (male)	0.723	0.309–1.689	0.454
Solid portion size on CT (per 1 cm increase)	4.352	2.333–8.121	<0.001
Solid portion size on CT			
Size ≤ 1 cm	Ref		
1 cm < size ≤ 2 cm	10.033	1.271–79.194	0.029
2 cm < size	28.693	3.772–218.238	0.001
CT lesion type			
Pure GGN or GGO-dominant PSN (reference)	Ref		
Solid-dominant PSN	5.653	0.696–45.949	0.105
Pure solid nodule	22.824	3.026–172.147	0.002
Histologic grade on the conventional classification			
Intermediate grade (reference)	Ref		
Low grade	0.057	0.003–1.020	0.052
High grade	2.298	0.717–7.367	0.162
Histologic grade on the updated classification			
Grade 2 (reference)	Ref		
Grade 1	0.083	0.004–1.531	0.0941
Grade 3	3.159	1.404–7.110	0.0054
Pathologic tumor size			
0 < tumor size ≤ 1 cm	0.091	0.005–1.741	0.1115
1 cm < tumor size ≤ 2 cm (reference)	Ref		
2 cm < tumor size	2.713	1.123–6.556	0.0266
Pathologic tumor size (per 1 cm increase)	2.432	1.588–3.726	<0.0001

CI: confidence interval; CT: computed tomography, GGN, ground-glass nodule; GGO: ground-glass opacity; HR, hazard ratio; PSN: part-solid nodule.

predominant histologic subtypes were reclassified as grade 3 in our study, which is in line with the results of previous studies [24,26].

Considering the significant contribution of the reclassified tumors to prognostic stratification, acknowledgment of the tumor characteristics of these lesions and non-invasive preoperative prediction could be of clinical interest. Despite the previous validation studies of updated systems, the association between CT characteristics and new histologic grades and imaging characteristics of lung adenocarcinomas with > 20% high-grade patterns have not been well investigated. Nevertheless, the association of CT characteristics (e.g., GGO proportion, solid portion size, or CT lesion type) with the predominant histologic subtype has been investigated in previous studies [12,16,27,28]. Generally, GGO in lung adenocarcinomas manifesting as pure GGNs or PSNs on CT reflects the lepidic component of the tumor. In contrast, the solid portion in CT correlates well with non-lepidic, invasive components. Therefore, lepidic-predominant adenocarcinomas mostly present as pure GGNs or GGO-dominant PSNs, whereas lesions with non-lepidic predominant

Table 5
Comparison of the c-index and iAUC between the prognostic prediction models for recurrence-free survival.

	Difference for c-index (95% CI)	Difference for iAUC (95% CI)
Model 1 vs. Model 2	**−0.031(-0.111, −0.003)**	**−0.02(-0.062, −0.004)**
Model 1 vs. Model 3	**−0.08(-0.158, −0.022)**	**−0.065(-0.139, −0.016)**
Model 1 vs. Model 4	**−0.092(-0.178, −0.003)**	−0.079(-0.164, 0.008)
Model 2 vs. Model 3	−0.049(-0.116, 0.009)	−0.046(-0.106, 0.001)
Model 2 vs. Model 4	−0.061(-0.146, 0.037)	−0.06(-0.142, 0.023)
Model 3 vs. Model 4	−0.012(-0.097, 0.08)	−0.014(-0.094, 0.067)

Bolds indicate statistical significance. CI: confidence interval; iAUC: integrated area under the curve.

Table 4
Multivariable Cox hazard models for the predictors of recurrence-free survival.

	HR	95% CI	P value	C-index (95% CI)	iAUC (95% CI)
Model 1 (pathologic tumor size)				0.723 (0.652–0.792)	0.731 (0.663–0.796)
Pathologic tumor size					
0 < tumor size ≤ 1 cm	0	0-inf			
1 cm < tumor size ≤ 2 cm (reference)	Ref				
2 cm < tumor size	2.824	1.171–6.813	0.0209		
Model 2 (pathologic tumor size + histologic grade on the conventional system)				0.754 (0.684–0.82)	0.751 (0.69–0.81)
Pathologic tumor size					
0 < tumor size ≤ 1 cm	0	0-inf			
1 cm < tumor size ≤ 2 cm (reference)	Ref				
2 cm < tumor size	2.644	1.093–6.392	0.0309		
Histologic grade on the conventional grading system					
Intermediate grade (reference)	Ref				
Low grade	0	0-inf			
High grade	1.975	0.587–6.645	0.2714		
Model 3 (pathologic tumor size + histologic grade on the updated grading system)				0.803 (0.734–0.864)	0.796 (0.733–0.857)
Pathologic tumor size					
0 < tumor size ≤ 1 cm	0	0-inf			
1 cm < tumor size ≤ 2 cm (reference)	Ref				
2 cm < tumor size	2.700	1.119–6.515	0.0271		
Histologic grade on the updated grading system					
Grade 2 (reference)	Ref				
Grade 1	0	0-inf			
Grade 3	3.303	1.479–7.378	0.0036		
Model 4 (solid portion size on CT + CT lesion type)				0.815 (0.739, 0.884)	0.81 (0.736, 0.879)
CT solid size					
Size ≤ 1 cm	Ref				
1 cm < size ≤ 2 cm	5.179	0.398–67.428	0.209		
2 cm < size	12.722	0.937–172.676	0.056		
CT lesion type					
Pure GGN and GGO dominant PSN (reference)	Ref				
Solid dominant PSN	1.325	0.099–17.736	0.831		
Pure solid nodule	4.042	0.301–54.268	0.292		

CI: confidence interval; CT: computed tomography, GGN, ground-glass nodule; GGO: ground-glass opacity; HR, hazard ratio; PSN: part-solid nodule.

histologic subtypes present as solid-dominant PSNs or pure solid nodules. Because the updated grading system has been developed based on the predominant histologic subtype and the presence of > 20% high-grade subtypes, the known relationship between CT features and predominant histologic subtypes in lung adenocarcinomas would be partly valid. In our study, histologic grades on the updated grading system showed a significant association with CT lesion type, and tumors with higher grades tended to have large solid portions on CT. Among grade 2 tumors (acinar or papillary) on the conventional system, the larger solid portion on CT may reflect the presence of a high-grade pattern > 20%. Because CT characteristics are significantly associated with histologic subtype grading, the model combined with CT parameters (pathologic stage plus CT lesion type) can show a comparable prognostic value in predicting the RFS in comparison with pathology-based prognostic models.

Our study had several limitations. First, it was a retrospective and single-center study, which limited the generalizability of our results. Second, further detailed qualitative or quantitative analyses with more abundant features (e.g., radiomics) could be helpful for the prediction of histologic grades and better performance of CT imaging-based prognostic models.

5. Conclusion

The 2020 IASLC histologic grading system, along with the conventional histologic grading system, has significant incremental prognostic value over the established prognostic factors in surgically resected pathologic stage 1 lung adenocarcinomas. Invasive lung adenocarcinomas that are reclassified as a higher category on the updated grading system have a larger solid proportion and a higher percentage of lesion type as pure solid nodules on preoperative CT.

CRediT authorship contribution statement

In Sung Cho: Formal analysis, Writing – original draft. **Hyo Sup Shim:** Investigation, Writing – review & editing. **Hye-Jeong Lee:** Investigation, Writing – review & editing. **Young Joo Suh:** Conceptualization, Methodology, Validation, Resources, Writing – original draft, Writing – review & editing, Project administration, Funding acquisition.

Declaration of Competing Interest

The authors declare that they have no known competing financial interests or personal relationships that could have appeared to influence the work reported in this paper.

Acknowledgements

None.

Funding

This work was supported by a faculty research grant of Yonsei University College of Medicine (6-2020-0209).

Appendix A. Supplementary material

Supplementary data to this article can be found online at https://doi.org/10.1016/j.lungcan.2023.107345.

References

[1] A. Jemal, K.C. Chu, R.E. Tarone, Recent trends in lung cancer mortality in the United States, J. Natl. Cancer Inst. 93 (4) (2001) 277–283, https://doi.org/10.1093/jnci/93.4.277.

[2] A. Shin, C.M. Oh, B.W. Kim, H. Woo, Y.J. Won, J.S. Lee, Lung Cancer Epidemiology in Korea, Cancer Res. Treat. 49 (3) (2017) 616–626, https://doi.org/10.4143/crt.2016.178.

[3] Y. Toyoda, T. Nakayama, A. Ioka, H. Tsukuma, Trends in lung cancer incidence by histological type in Osaka, Japan, Jpn. J. Clin. Oncol. 38 (8) (2008) 534–539, https://doi.org/10.1093/jjco/hyn072.

[4] R. Rami-Porta, V. Bolejack, P. Goldstraw, The new tumor, node, and metastasis staging system, Semin. Respir. Crit. Care Med. 32 (1) (2011) 44–51, https://doi.org/10.1055/s-0031-1272868.

[5] A. Warth, T. Muley, M. Meister, A. Stenzinger, M. Thomas, P. Schirmacher, P. A. Schnabel, J. Budczies, H. Hoffmann, W. Weichert, The novel histologic International Association for the Study of Lung Cancer/American Thoracic Society/European Respiratory Society classification system of lung adenocarcinoma is a stage-independent predictor of survival, J. Clin. Oncol. 30 (13) (2012) 1438–1446, https://doi.org/10.1200/JCO.2011.37.2185.

[6] Z. Sun, M.C. Aubry, C. Deschamps, R.S. Marks, S.H. Okuno, B.A. Williams, H. Sugimura, V.S. Pankratz, P. Yang, Histologic grade is an independent prognostic factor for survival in non-small cell lung cancer: an analysis of 5018 hospital- and 712 population-based cases, J. Thorac. Cardiovasc. Surg. 131 (5) (2006) 1014–1020, https://doi.org/10.1016/j.jtcvs.2005.12.057.

[7] W.D. Travis, E. Brambilla, M. Noguchi, A.G. Nicholson, K.R. Geisinger, Y. Yatabe, D.G. Beer, C.A. Powell, G.J. Riely, P.E. Van Schil, K. Garg, J.H. Austin, H. Asamura, V.W. Rusch, F.R. Hirsch, G. Scagliotti, T. Mitsudomi, R.M. Huber, Y. Ishikawa, J. Jett, M. Sanchez-Cespedes, J.P. Sculier, T. Takahashi, M. Tsuboi, J. Vansteenkiste, I. Wistuba, P.C. Yang, D. Aberle, C. Brambilla, D. Flieder, W. Franklin, A. Gazdar, M. Gould, P. Hasleton, D. Henderson, B. Johnson, D. Johnson, K. Kerr, K. Kuriyama, J.S. Lee, V.A. Miller, I. Petersen, V. Roggli, R. Rosell, N. Saijo, E. Thunnissen, M. Tsao, D. Yankelewitz, International association for the study of lung cancer/american thoracic society/european respiratory society international multidisciplinary classification of lung adenocarcinoma, J. Thoracic Oncol.: Offic. Publ. Int. Assoc. Study Lung Cancer 6 (2) (2011) 244–285, https://doi.org/10.1097/JTO.0b013e318206a221.

[8] P.A. Russell, Z. Wainer, G.M. Wright, M. Daniels, M. Conron, R.A. Williams, Does lung adenocarcinoma subtype predict patient survival?: A clinicopathologic study based on the new International Association for the Study of Lung Cancer/American Thoracic Society/European Respiratory Society international multidisciplinary lung adenocarcinoma classification, J. Thorac. Oncol. 6 (9) (2011) 1496–1504, https://doi.org/10.1097/JTO.0b013e318221f701.

[9] A. Yoshizawa, N. Motoi, G.J. Riely, C.S. Sima, W.L. Gerald, M.G. Kris, B.J. Park, V. W. Rusch, W.D. Travis, Impact of proposed IASLC/ATS/ERS classification of lung adenocarcinoma: prognostic subgroups and implications for further revision of staging based on analysis of 514 stage I cases, Mod. Pathol. 24 (5) (2011) 653–664, https://doi.org/10.1038/modpathol.2010.232.

[10] A.L. Moreira, P.S.S. Ocampo, Y. Xia, H. Zhong, P.A. Russell, Y. Minami, W.A. Cooper, A. Yoshida, L. Bubendorf, M. Papotti, G. Pelosi, F. Lopez-Rios, K. Kunitoki, D. Ferrari-Light, L.M. Sholl, M.B. Beasley, A. Borczuk, J. Botling, E. Brambilla, G. Chen, T.Y. Chou, J.H. Chung, S. Dacic, D. Jain, F.R. Hirsch, D. Hwang, S. Lantuejoul, D. Lin, J.W. Longshore, N. Motoi, M. Noguchi, C. Poleri, N. Rekhtman, M.S. Tsao, E. Thunnissen, W.D. Travis, Y. Yatabe, A.C. Roden, J.B. Daigneault, Wistuba, II, K.M. Kerr, H. Pass, A.G. Nicholson, M. Mino-Kenudson, A Grading System for Invasive Pulmonary Adenocarcinoma: A Proposal From the International Association for the Study of Lung Cancer Pathology Committee, J. Thoracic Oncol.: Offic. Publ. Int. Assoc. Study Lung Cancer 15 (10) (2020) 1599–1610. 10.1016/j.jtho.2020.06.001.

[11] E.J. Hwang, C.M. Park, Y. Ryu, S.M. Lee, Y.T. Kim, Y.W. Kim, J.M. Goo, Pulmonary adenocarcinomas appearing as part-solid ground-glass nodules: is measuring solid component size a better prognostic indicator? Eur. Radiol. 25 (2) (2015) 558–567, https://doi.org/10.1007/s00330-014-3441-1.

[12] Y. Kudo, J. Matsubayashi, H. Saji, S. Akata, Y. Shimada, Y. Kato, M. Kakihana, N. Kajiwara, T. Ohira, T. Nagao, N. Ikeda, Association between high-resolution computed tomography findings and the IASLC/ATS/ERS classification of small lung adenocarcinomas in Japanese patients, Lung Cancer 90 (1) (2015) 47–54, https://doi.org/10.1016/j.lungcan.2015.07.007.

[13] Y. Tsutani, Y. Miyata, T. Yamanaka, H. Nakayama, S. Okumura, S. Adachi, M. Yoshimura, M. Okada, Solid tumors versus mixed tumors with a ground-glass opacity component in patients with clinical stage IA lung adenocarcinoma: prognostic comparison using high-resolution computed tomography findings, J. Thorac. Cardiovasc. Surg. 146 (1) (2013) 17–23, https://doi.org/10.1016/j.jtcvs.2012.11.019.

[14] H. Uehara, Y. Tsutani, S. Okumura, H. Nakayama, S. Adachi, M. Yoshimura, Y. Miyata, M. Okada, Prognostic role of positron emission tomography and high-resolution computed tomography in clinical stage IA lung adenocarcinoma, Ann. Thorac. Surg. 96 (6) (2013) 1958–1965, https://doi.org/10.1016/j.athoracsur.2013.06.086.

[15] Y. Tsutani, Y. Miyata, H. Nakayama, S. Okumura, S. Adachi, M. Yoshimura, M. Okada, Prognostic significance of using solid versus whole tumor size on high-resolution computed tomography for predicting pathologic malignant grade of tumors in clinical stage IA lung adenocarcinoma: a multicenter study, J. Thorac. Cardiovasc. Surg. 143 (3) (2012) 607–612, https://doi.org/10.1016/j.jtcvs.2011.10.037.

[16] Y.J. Suh, H.J. Lee, Y.T. Kim, C.H. Kang, I.K. Park, Y.K. Jeon, D.H. Chung, Added prognostic value of CT characteristics and IASLC/ATS/ERS histologic subtype in surgically resected lung adenocarcinomas, Lung Cancer 120 (2018) 130–136, https://doi.org/10.1016/j.lungcan.2018.04.007.

[17] M. Rokutan-Kurata, A. Yoshizawa, K. Ueno, N. Nakajima, K. Terada, M. Hamaji, M. Sonobe, T. Menju, H. Date, S. Morita, H. Haga, Validation Study of the

International Association for the Study of Lung Cancer Histologic Grading System of Invasive Lung Adenocarcinoma, J. Thorac. Oncol. 16 (10) (2021) 1753–1758, https://doi.org/10.1016/j.jtho.2021.04.008.

[18] C. Deng, Q. Zheng, Y. Zhang, Y. Jin, X. Shen, X. Nie, F. Fu, X. Ma, Z. Ma, Z. Wen, S. Wang, Y. Li, H. Chen, Validation of the Novel International Association for the Study of Lung Cancer Grading System for Invasive Pulmonary Adenocarcinoma and Association With Common Driver Mutations, J. Thoracic Oncol.: Offic. Publ. Int. Assoc. Study Lung Cancer 16 (10) (2021) 1684–1693, https://doi.org/10.1016/j.jtho.2021.07.006.

[19] S. Chang, J. Hur, Y.J. Hong, H.J. Lee, Y.J. Kim, K. Han, B.W. Choi, Adverse Prognostic CT Findings for Patients With Advanced Lung Adenocarcinoma Receiving First-Line Epidermal Growth Factor Receptor-Tyrosine Kinase Inhibitor Therapy, AJR Am. J. Roentgenol. 210 (1) (2018) 43–51, https://doi.org/10.2214/AJR.17.18167.

[20] E.A. Park, H.J. Lee, Y.T. Kim, C.H. Kang, K.W. Kang, Y.K. Jeon, J.M. Goo, C.H. Lee, C.M. Park, EGFR gene copy number in adenocarcinoma of the lung by FISH analysis: investigation of significantly related factors on CT, FDG-PET, and histopathology, Lung Cancer 64 (2) (2009) 179–186, https://doi.org/10.1016/j.lungcan.2008.08.003.

[21] W.D. Travis, E. Brambilla, A.G. Nicholson, Y. Yatabe, J.H.M. Austin, M.B. Beasley, L.R. Chirieac, S. Dacic, E. Duhig, D.B. Flieder, K. Geisinger, F.R. Hirsch, Y. Ishikawa, K.M. Kerr, M. Noguchi, G. Pelosi, C.A. Powell, M.S. Tsao, I. Wistuba, The 2015 World Health Organization Classification of Lung Tumors: Impact of Genetic, Clinical and Radiologic Advances Since the 2004 Classification, J. Thoracic Oncol.: Offic. Publ. Int. Assoc. Study Lung Cancer 10 (9) (2015) 1243–1260.

[22] P. Goldstraw, K. Chansky, J. Crowley, R. Rami-Porta, H. Asamura, W.E. Eberhardt, A.G. Nicholson, P. Groome, A. Mitchell, V. Bolejack, S. International Association for the Study of Lung Cancer, A.B. Prognostic Factors Committee, I. Participating, S. International Association for the Study of Lung Cancer, B. Prognostic Factors Committee Advisory, I. Participating, The IASLC Lung Cancer Staging Project: Proposals for Revision of the TNM Stage Groupings in the Forthcoming (Eighth) Edition of the TNM Classification for Lung Cancer, J. Thorac. Oncol., 11 (1) (2016) 39–51. 10.1016/j.jtho.2015.09.009.

[23] W. Woo, Y.J. Cha, B.J. Kim, D.H. Moon, S. Lee, Validation Study of New IASLC Histology Grading System in Stage I Non-Mucinous Adenocarcinoma Comparing With Minimally Invasive Adenocarcinoma, Clin. Lung Cancer 23 (7) (2022), https://doi.org/10.1016/j.cllc.2022.06.004 e435-e442.

[24] L. Xu, H. Su, L. Hou, F. Wang, H. Xie, Y. She, J. Gao, S. Zhao, C. Dai, D. Xie, Y. Zhu, C. Wu, D. Zhao, C. Chen, G. Surgical Thoracic Alliance of Rising Star, The IASLC Proposed Grading System Accurately Predicts Prognosis and Mediastinal Nodal Metastasis in Patients With Clinical Stage I Lung Adenocarcinoma, Am. J. Surg. Pathol., 46 (12) (2022) 1633–1641. 10.1097/PAS.0000000000001876.

[25] N. Yanagawa, M. Sugai, S. Shikanai, R. Sugimoto, M. Osakabe, N. Uesugi, H. Saito, M. Maemondo, T. Sugai, The new IASLC grading system for invasive non-mucinous lung adenocarcinoma is a more useful indicator of patient survival compared with previous grading systems, J. Surg. Oncol. (2022), https://doi.org/10.1002/jso.27091.

[26] Y. Choi, J. Kim, H. Park, H.K. Kim, J. Kim, J.Y. Jeong, J.H. Ahn, H.Y. Lee, Rethinking a Non-Predominant Pattern in Invasive Lung Adenocarcinoma: Prognostic Dissection Focusing on a High-Grade Pattern, Cancers (Basel) 13 (11) (2021), https://doi.org/10.3390/cancers13112785.

[27] J.P. Ko, J. Suh, O. Ibidapo, J.G. Escalon, J. Li, H. Pass, D.P. Naidich, B. Crawford, E. B. Tsai, C.W. Koo, A. Mikheev, H. Rusinek, Lung Adenocarcinoma: Correlation of Quantitative CT Findings with Pathologic Findings, Radiology 280 (3) (2016) 931–939, https://doi.org/10.1148/radiol.2016142975.

[28] M.J. Cha, H.Y. Lee, K.S. Lee, J.Y. Jeong, J. Han, Y.M. Shim, H.S. Hwang, Micropapillary and solid subtypes of invasive lung adenocarcinoma: clinical predictors of histopathology and outcome, J. Thorac. Cardiovasc. Surg., 147 (3) (2014) 921-928 e922. 10.1016/j.jtcvs.2013.09.045.